U–Pb and Sm–Nd geochronology of amphibolites from the Curaçá Belt, São Francisco Craton, Brazil: Tectonic implications

Luiz José Homem D'el-Rey Silva - Universidade de Brasília — Instituto de Geociências
Elton Luiz Dantas - Laboratório de Geocronologia, Universidade de Brasília
João Batista Guimarães Teixeira - Grupo de Metalogênese, Centro de Pesquisa em Geofísica e Geologia, Universidade Federal da Bahia, Campus Universitário de Ondina, Sala **Jorge Henrique Laux** - Laboratório de Geocronologia, Universidade de Brasília
Maria da Glória da Silva - Grupo de Metalogênese, Centro de Pesquisa em Geofísica e Geologia, Universidade Federal da Bahia, Campus Universitário de Ondina e Serviço Geológico do Brasil (CPRM)

Abstract

The Curaçá terrane is part of the Itabuna–Salvador–Curaçá (I–S–C) Paleoproterozoic orogen in the São Francisco craton, northeastern Brazil, and comprises supracrustal rocks, gneisses of their probable basement, amphibolites, and mafic-ultramafic Cu-bearing bodies (including the Caraíba Cu-Mine), all affected by D1-D3 deformation events associated to M1-M3 metamorphism under high-T granulite and amphibolite facies, and assisted by G1-G3 tonalitic-granodioritic-granitic intrusions. U–Pb and Sm–Nd Thermal Ionization Mass Spectrometry (TIMS) isotopic data from amphibolite, tonalite, and granite, sampled in a well-known outcrop, indicate partial reset and heterogeneous modification of the original isotopic systems, attributable to deformation and metamorphism. The ages obtained from these systems agree with each other, and also with other previously published U–Pb data, and imply that 2.6 Ga is the crystallization age of the protolith of the amphibolite. Together with key structural relationships, they also indicate a 2.08–2.05 Ga interval for M3 metamorphism, and make even a less precise age (2.2–2.3 Ga) acceptable, as it suggests contamination in the amphibolite with material in a syn-D2 tonalite crystallized 2248±36 Ma ago. The new data demonstrate the existence of Neoarchean fragments of both oceanic and continental crusts and constrain the Archean-Paleoproterozoic development of the Curaçá belt, the I–S–C orogen, and the São Francisco craton.

Keywords: U–Pb and Sm–Nd isotopic data; Curaçá terrane; São Francisco craton; Archean to Paleoproterozoic tectonics; Caraíba Mine

1. Introduction

Proterozoic mobile belts or terranes of high metamorphic grade are among the most characteristic features of continental shield areas (Windley, 1986; Condie, 1989). These terranes consist of polydeformed/metamorphosed rocks displaying a generally older regional metamorphic banding that may hide the evidence for polycyclic tectonic events recognisable only upon detailed mapping combined with lithogeochemistry (Passchier et al., 1990). Consequently accurate dating of protoliths crystallization and/or deformation and metamorphism in such belts relies on detailed structural studies of key outcrops combined with geochronological methods (Gromet, 1991). The Curaçá River Valley terrane is the N–S trending northern segment of the Itabuna–Salvador–Curaçá (I–S–C) Paleoproterozoic orogenic belt that stretches between the Mesoarchean Gavião, Serrinha, and Jequié cratonic blocks, in the central-eastern part of the São Francisco craton, Bahia, eastern Brazil (Fig. 1; Sabaté et al., 1990; Barbosa et al., 1996). The existence of reworked Archean rocks in the Curaçá terrane (Inda and Barbosa, 1978; Lindenmayer, 1981), and across the entire I–S–C orogen, has driven Leite (2002) and Barbosa and Sabaté (2002, 2004) to postulate the participation of a fourth Archean block inside the Paleoproterozoic collision zone. Geodynamic models for the Archean-Paleoproterozoic evolution of the São Francisco craton have been supported by recent isotopic studies (Oliveira et al., 2004; Barbosa and Sabaté, 2004), indicating that the I–S–C orogen and the three Archean blocks preserve distinct Sm–Nd characteristics (Fig. 1a).

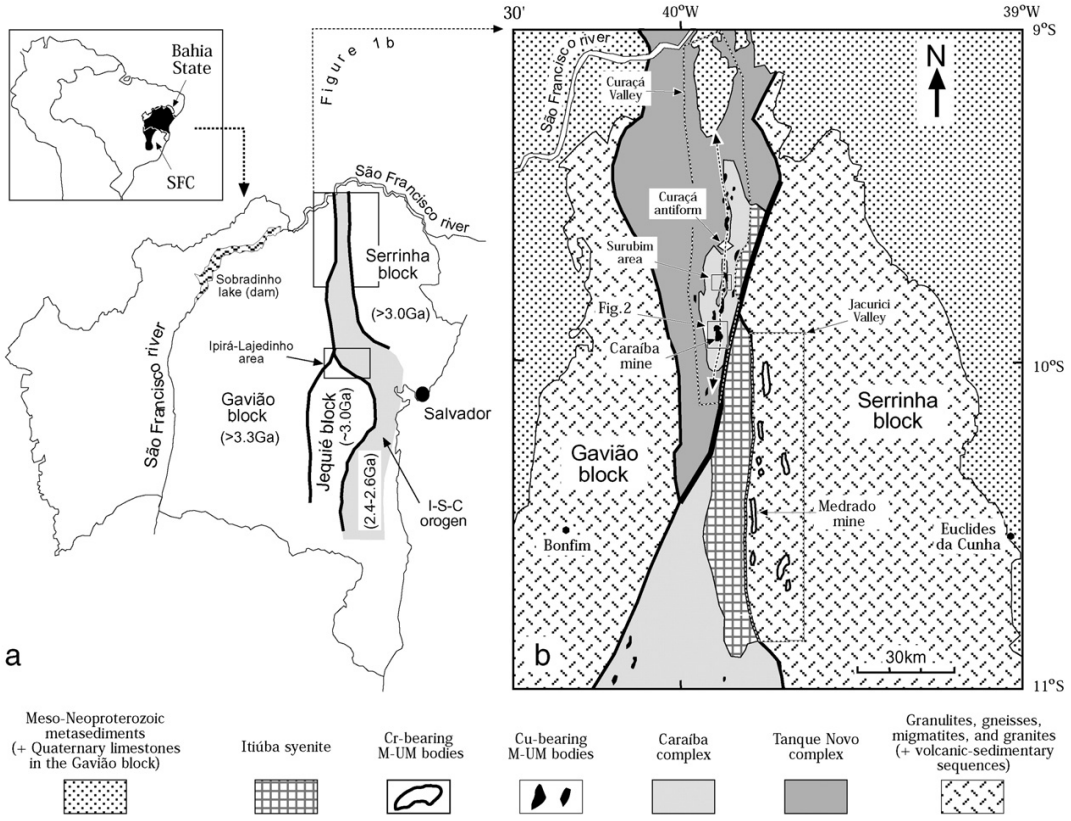

Fig. 1. a - Summary display of the Gavião, Serrinha and Jequié blocks, and the Itabuna–Salvador–Curaçá (I–S–C) orogen, all within the geographical limits of the of the Bahia State, and part of the São Francisco craton, Brazil. Numbers in brackets represent TDM model age data for each block (adapted from Barbosa and Sabaté, 2004). b—Simplified geological map of the part of northern Bahia to show the northern part of the I–S–C orogen (=Curaçá terrane), between the Gavião and the Serrinha Archean blocks (combining Figs. 1 in D'el-Rey Silva, 1984, 1985; and in Oliveira et al., 2004). The Caraíba orebody and the area of Fig. 2 are highlighted. Details in text.

Early regional studies (Delgado and Souza, 1975) made the Curaçá terrane well-known because of its high potential for Cusulphide mineralization associated with mafic–ultramafic (M– UM) bodies mapped within high metamorphic grade supracrustal rocks (metasediments and metavolcanics), gneisses, migmatites, and metagranitoids. In fact, following the accidental discovery of green copper oxide (malachite) nearly 140 years ago in the site destined to become the Caraíba Mine (Fig. 1b), six other smaller Cu-deposits have been found in the two last decades, among over two hundred small bodies (D'el-Rey Silva, 1984, 1985). Structures record progressive (D1-D3) deformation (Fig. 2; D'el-Rey Silva, 1993) and conditions for the main metamorphism have been estimated around 850°– 720 °C (Jardim de Sá et al., 1982; Ackermand et al., 1987), or up to 1000 °C, with pressures varying from 8–10 kbar (Leite, 2002; Leite et al., 2005), all on the basis of several geothermometers and sapphirine-bearing assemblages. The first U–Pb isotopic data for rocks of the Curaçá belt, all from the surroundings of the Caraíba orebody (Fig. 2), indicated crystallization ages of: 2580±10 Ma for a sample of norite collected at the Caraíba Mine (U–Pb Sensitive High Resolution Ion Microprobe – SHRIMP – data in Oliveira et al., 2004); 2248±36Ma for

syn-D2 tonalite in the Caraíba Airport outcrop; and 2051±16 Ma for syn-D3 granite intrusive in the Caraíba orebody (both U–Pb data, but respectively from zircons and monazite; D'el-Rey Silva et al., 1996), whereas the age of the supracrustals was not directly determined. This paper presents the results of U–Pb and Sm–Nd integrated studies carried out on samples of amphibolite, tonalite and granite of the Caraíba Airport outcrop, situated ~5 km to the north of the Caraíba orebody (Fig. 2). This outcrop is one of the most visited places in the Curaçá belt exactly because it displays clear evidence for a D1-D3 progressive deformation under M1-M3 metamorphism, providing a well-constrained structural-metamorphic framework for targeting geochronological studies.

2. Regional geology and tectonic setting

The basement of the São Francisco Craton is mostly represented by the Gavião and Serrinha blocks, shown respectively to the west and to the east of the Curaçá terrane, in their simplest map expression (Fig. 1b). The Gavião block is mainly composed of gneiss-amphibolite associations, amphibolite-facies tonalite-granodiorite orthogneisses dated at 2800–2900 Ma as well as greenstone belts. The block also encloses a 3200–3400 Ma trondhjemite-tonalite-granodiorite suite (Barbosa and Sabaté, 2004). Its westernmost part is covered by (meta) sediments deformed in the Neoproterozoic Brasiliano orogeny and by Quaternary limestones, whereas the eastern part includes (to the west of the town of Bonfim, Fig. 1b) the Campo Formoso Cr-bearing mafic–ultramafic layered body, a major intrusion that is unconformably overlain by the Jacobina Group, both of which are intruded by the Late Paleoproterozoic Campo Formoso granite (Silva, 1996; Leite, 2002). According to a summary in Silva (1996) the Jacobina Group is part of a much longer Paleoproterozoic rift-like volcanic-sedimentary basin extending to the boundary between the Gavião and Jequié blocks. The Serrinha block consists of amphibolite-facies 2900–3500 Ma ortho and paragneisses of granodiorite composition, as well as migmatites and amphibolites (Barbosa and Sabaté, 2004). The western margin is in contact with the Itiúba syenite, whereas the eastern margin encloses Paleoproterozoic greenstone sequences, and arc-like orthogneiss and granites that are indicators of a back-arc basin system within the Serrinha block (Silva, 1996). Farther to the east, this block underlies Neoproterozoic (meta)sediments

and, outside of Fig. 1b, Mesozoic sediments of the Tucano basin. The I–S–C orogen (Fig. 1) is mainly composed of granulitefacies tonalitic and charnockitic rocks with basic-ultrabasic enclaves, as well as supracrustal rocks, in both of its northern and southern segments (Barbosa and Sabaté, 2004). The 2084 Ma old Itiúba syenite separates the 2580 Ma old Curaçá Valley Cu-district to the west, from the 2085 Ma old Jacurici Valley Cr-district to the east (Fig. 1b; all U–Pb SHRIMP age of zircons; Oliveira et al., 2004).

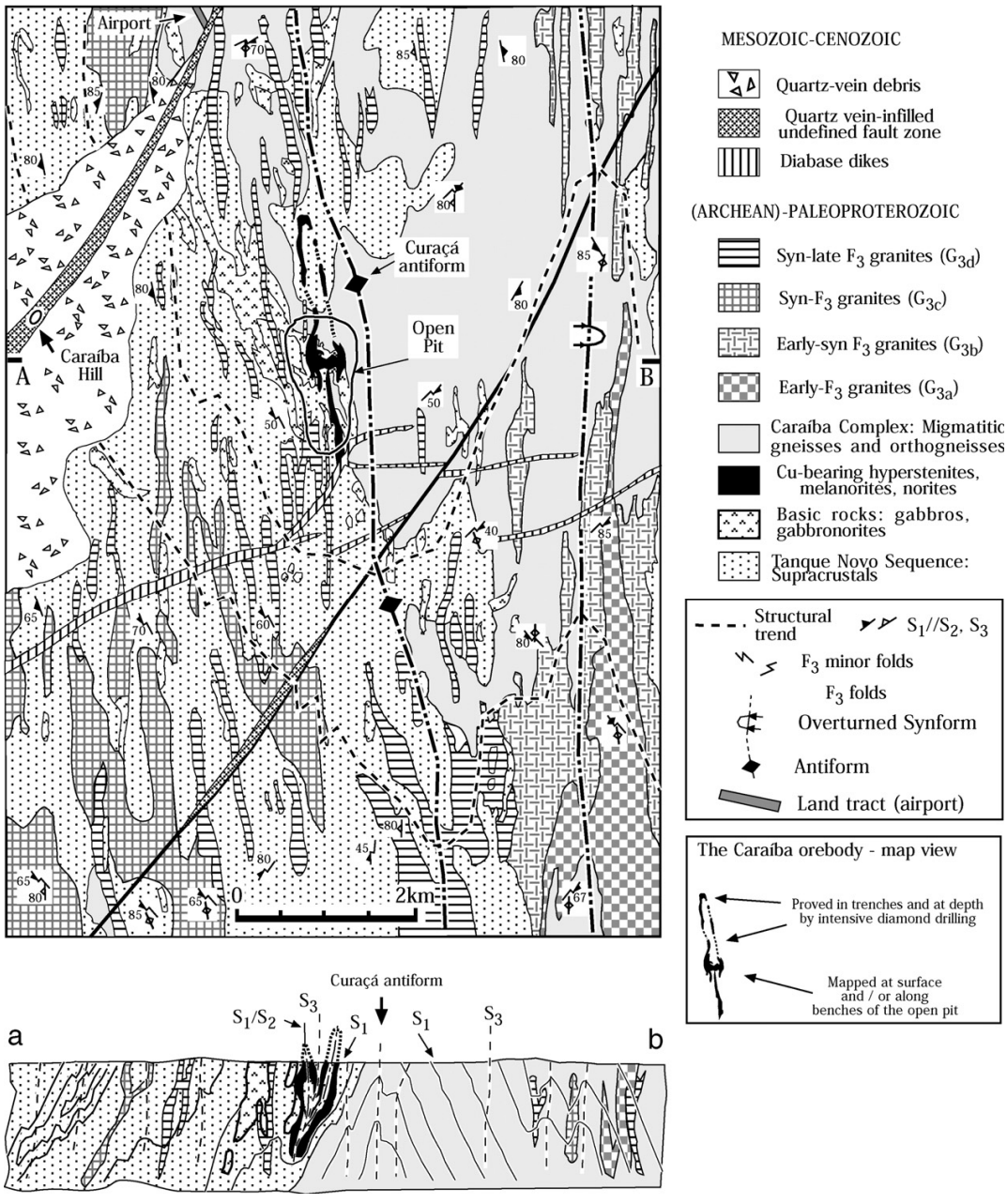

Fig. 2. Simplified geological map of the area surrounding the Caraíba orebody, highlighting the Curaçá antiform, the open pit, and the land track of the airport. Based on a 1:10,000 scale geological mapping carried out by D'el-Rey Silva (1984, 1985) along 130 km of E–W

tracks distributed in 18 lines 500 m apart one from each other, some marked every 100 m, others marked every 50 m, a real frame (omitted for simplicity) opened in the field for geophysical survey. Mapping of the orebody itself was at 1:1,000 scale (see Fig. 3a) whereas the part to the N of the open pit (belonging to DOCEGEO Company) was mapped at 1:5,000 scale (Lindenmayer et al., 1984). See details in text.

3. Regional geology of the Curaçá high-grade terrane

3.1. Lithostratigraphy

The lithotypes of the Curaçá terrane are divided into the Tanque Novo and Caraíba complexes, both including the Cubearing mafic-ultramafic bodies (Fig. 1b). The Tanque Novo Complex comprises Al-rich paragneisses, banded gneisses, calcsilicate rocks, quartzites, iron formations and graphite gneisses, whereas the Caraíba complex comprises mostly enderbitic and charnocktic orthogneisses, as well as migmatites. Most of the regional geology and structural evolution of the Curaçá belt (Lindenmayer, 1981; Figueiredo, 1981; Mandetta, 1982; Gáal, 1982; Hasuy et al., 1982; Jardim de Sá et al., 1982; D'el-Rey Silva, 1984, 1985), published at the same time or soon after the start-up of the Caraíba Mine operation, have shown the Curaçá terrane as formed of three main lithostratigraphic units also recorded in the vicinities of the Caraíba orebody (Fig. 2), the area submitted to the most detailed mapping carried out in the Curaçá belt. The Tanque Novo Complex is a supracrustal sequence consisting mostly of quartzofeldspathic gneiss with thin intercalations of amphibolites, cordierite-sillimanite-garnet paragneiss, oxide-facies banded iron formation, calcsilicate rocks, anhydrate-bearing marbles, forsterite-marbles and quartzites, as well as gneisses supposed to belong, at least in part, to the crystalline basement. The second unit consists of Cu-poor or simply barren gabbros, gabbronorites, leucogabbros, and hyperites, together with Cu-rich hypersthenites, melanorites, and norites. A vast amount of geology and structural data collected regionally, and also on surface and in underground sites of the Caraíba Mine and other small bodies, drove Lindenmayer (1981), Lindenmayer et al. (1984), D'el-Rey Silva (1984, 1985), and lately Mayer and Barnes (1996) and D'el-Rey Silva et al. (1988, 1994, 1996) to state that the Cu-bearing rocks are sill-like structures. It is noteworthy that the Caraíba orebody is a Cu-only, chalcopyrite and bornite-rich deposit and associated with deep ocean rocks such as banded iron formation and evaporites (anhydrate)

forsterite-marble. The third unit (the Caraíba complex) mostly comprises migmatitic gneisses and syntectonic intrusions (G1 and G2) generally consisting of grey tonalites and granodiorites. Reddish-pink coloured, K-rich (G3) granites intruded all lithotypes and developed in association with D3 (Fig. 2).

3.2. Structures and metamorphism

The Curaçá belt has been affected by a D1-D3 progressive deformation assisted by large volumes of syntectonic G1-G3 granitoid intrusions. Associated metamorphisms M2 (granulite facies) and M3 (amphibolite facies) are quite evident everywhere, but evidence for a M1 amphibolite facies metamorphism is solely preserved in paragneisses and amphibolites that occur as dm- to m-scale boudins or xenoliths entrained in G2 intrusions across the belt (Jardim de Sá et al., 1982; D'el-Rey Silva, 1984, 1985).

Jardim de Sá et al. (1982) first reported M1 amphibolitefacies metamorphism on the basis of: 1 — Migmatites affected by D2 and D3 events; 2 — Biotite inclusions (M1) found in crystals of orthopyroxene (M2) in paragneisses; and 3 — An opx-rich border surrounding layers and boudins of mafic rocks (amphibolites) in paragneisses, all affected by F3 folds associated with M3 metamorphism (their Fig. 4H). Whereas these observations are respectively from outcrops to the south and north of Caraíba (the two latter in the Tanque Novo Sequence, Surubim area; Fig. 1b), the existence of M1 metamorphism in the Caraíba area (Fig. 2) is demonstrated by several inclusions of circular crystals of green hornblende in hypersthene from the opx-rich border of mafic boudins in the Airport outcrop (photograph 45, page 153 of D'el-Rey Silva's MSc thesis, 1984). Hypersthene-free amphibolites have been largely documented across the Curaçá Valley (modal compositions in page 99 of Lindenmayer, 1981). M2 mineral assemblages include cordierite-sillimanite-garnet-biotite in paragneisses, and andesine plus hypersthene (strongly pleochroic and rich in Al_2O_3) in commonly granoblastic gabbroic rocks, even the Cu-bearing bodies (Lindenmayer, 1981). M3 metamorphism resulted in the transformation of hypersthene into hornblende and biotite, in F3 hinges (photographs 50 and 51, D'el-Rey Silva's MSc thesis) and is characterized by biotite, hornblende, quartz and feldspar assemblages (Lindenmayer, 1981).

Due to D1-D3 evolution, the older metamorphic banding (S1) and intrafolial folds F1 are affected by two folding phases (F2 and F3), so that S1 is mostly a composite structure where evidences for M1 is commonly absent, but M2 and M3 assemblages dominate. S1 appears in most outcrops as a continuous banding traceable for 10 m, or more, and consisting of cm- to dm-thick bands of dark, more mafic (hornblende, biotite, pyroxene) minerals, and bands of light, more felsic minerals (feldspars and quartz, mostly). S1 may also appear as mm- to cm-thick, generally continuous in ≤1 m-scale, or somehow diffuse banding in metabasic rocks and amphibolites such as the ones in the studied outcrop. S1 is also a banding parallel to S0 defined by the intercalation of 10 cm- to 50 cmthick layers of acid gneiss (possibly meta-arkose and/or metarhyolite), amphibolite, pelitic paragneiss, marble, banded iron formation, and calcsilicate rocks.

F1 folds are generally of 10 cm-scale, rootless and intrafolial relative to S1 (S0), whereas the F2 folds (and foliation S2) are mostly seen in outcrops of gneisses and orthogneisses, together with examples of 10–100 cm-sized patterns indicative of Ramsay's (1967) Type 2 of F2×F3 fold interference pattern (Jardim de Sá et al., 1982; D'el-Rey Silva, 1984) but could be better understood only after detailed mapping of the Caraíba orebody and surrounding area (next section). F3 and S3 are also very common features in the Curaçá terrane. F3 folds are noncylindrical, cm- to km-sized, generally tight, asymmetric, Everging, and their axial planes trend nearly N–S and dip 70°–75°W. The F3 axes (B3) plunge generally less than 30°, either in a northerly or southerly direction. S3 is a typical mineral foliation mostly defined by biotite, hornblende, and strongly flattened quartz/feldspars, but the non-micaceous minerals display a prolate geometry and define a penetrative L3 mineral stretching lineation parallel to B3. Granites G3 are early- to late- D3 (Fig. 2) and intruded sub-parallel to the axial trace of F3 folds. They most commonly display the S3 foliation, and represent typical lithotypes due to M3 metamorphism (Fig. 2). The Curaçá antiform (Delgado and Souza, 1975; Gáal, 1982) is a D3 structure, the hinge of which plunges to the N or to the S (reference to the Surubim area) and is the site for most of the mafic–ultramafic bodies (Fig. 1b). Also in the Surubim area, Jardim de Sá et al. (1982) and Hasuy et al. (1982)

described 1 m- to 10 m-sized structures of Type 1 (domes and basins) interference pattern between the regional F3 folds and gentleopen, very local F4 folds that have no influence in the geometry and spatial distribution of the layers.

4. The Airport outcrop: key geological features preserved in an extremely deformed area

The Airport outcrop is a flat-lying exposure of tonalitic orthogneiss with an amoeboid surface area of nearly 1000 m2, and lies in the northern end of the land track of the Mine airport, and is situated in the western limb and close to the hinge of the Curaçá antiform, in a similarly structural position as the Caraíba orebody (Fig. 2). The orthogneiss also encloses tens of boudins of amphibolite, the whole set intruded by sub-vertical, sheet-like bodies of pink granites, and some quartz-feldspar veins. The outcrop itself displays important clues for understanding the critical role of early E–W trending structures, such as the F2 folds, in the evolution of the Curaçá terrane (next section), but a complete understanding of the importance of the outcrop, and the importance of dating the amphibolites (see Discussion) all demand an overview on the geology of the Caraíba orebody, where such F2 folds were fully mapped (Fig. 3a), and on the tectonic conditions prevailing in the I–S–C orogen.

D3 flattening was so strong and melt-assisted that the real geometry of some of the 10 cm- to 1 m-scale F2×F3 fold interference patterns seen in the Curacá terrane is often obscured by disrupted hinges, melts injection, and/or extreme ductile thinning. However, the large amount of data from detailed mapping of the orebody and its surroundings (1978–1984; D'el- Rey Silva, 1984, 1985) and from mine operation in the following 18 years (D'el-Rey Silva et al., 1988, 1994, 1996; D'el-Rey Silva and Oliveira, 1999) allows a picture to be constructed of the Caraíba Cu-deposit within the core of a 1000 m-high, tight, non-cylindrical F3 synform gently-moderately plunging to the S (a parasite fold of the Curaçá antiform). It acquired the shape of a N–S trending mushroom (Figs. 2 and 3a), due to the interference of the F3 synform with several F2 folds, so that the E–W trending and originally sub-horizontal F2 axis (B2) appears sub-vertical in the upper half of the orebody (Fig. 3b), and the pre-D3 attitude of

the layers also forces F3 fold axes to plunge steeply to the N solely in the central and very inner part of the mushroom. Thus, the orebody consists, to the S of section 32 and to the N of section 37 (Fig. 3b), of a mineralized layer affected by simple synform, whereas between sections 32 to 37 (the central and richer part) it displays repetitions of the same layer due to several F2 hinges affected by the F3 synform (Fig. 3c and inset).

The importance of the Airport outcrop and the Caraíba orebody rests in the preservation of key evidence exactly where the I–S–C orogen was squeezed to its narrowest map expression (Fig. 1a-b). Similar D1-D3 structures and their field relationships are found further south, where the orogen is wider (in the Ipirá-Lajedinho area, Fig. 1a). In that area, largely protected by the northern margin of the Jequié block, abundant, m- to dm-scale, E–W trending F2 folds associated with mapable, ductile, D1-related lateral ramps, N–S trending D3 transcurrent faults, as well as F2×F3 interference patterns, some as large as the Caraíba mushroom, justifies interpreting the orogen as the result of a long-lived, oblique collision-related sinistral transpressional orogen (D'el-Rey Silva, 1993; Barbosa, 1996), and the intensity of shortening peaks around Caraíba for two reasons: 1 — the area surrounding Caraíba lies 300 km away from the Jequié block; and 2—intrusion of the D2-related syenite most likely added to make even stronger the E–W compression responsible for the transposition of any pre-D3 structures that existed in the Caraíba region.

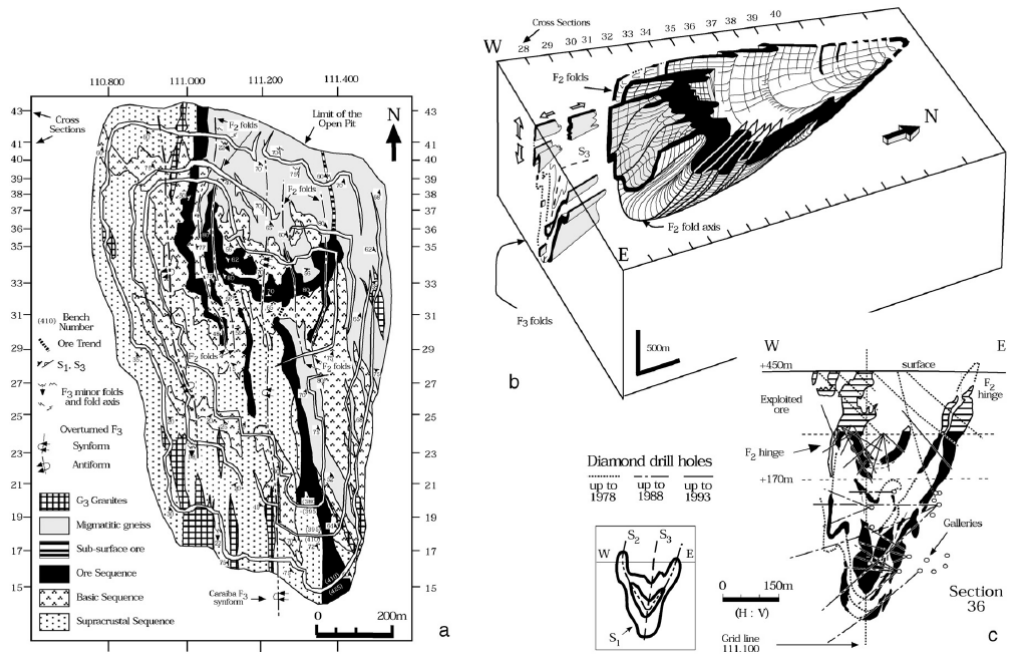

Fig. 3. a —Simplified geological map of the Caraíba orebody with indication of the S1 foliation, minor D3 structures, as well as the axial trace of the main F2 and F3 folds. The walls of each of the four upper benches of the open pit were mapped (1978–1984) in a 1:1,000 scale, simultaneously with the opening of bench 395 m, the lower one at that time, so the orebody could be tracked in great detail as new exposures were available every 10–20 m along strike, blast after blast. The geometry of the orebody match entirely the Cu-grade iso-contour map obtained on each bench by the plot of thousand data on the Cu-grade from drill holes of a 5 msquare grid used for blasting. The eastern limb of the mushroom structure occurs only underground, from cross section 35 to the N, and has been projected on surface as a modification here introduced in the original map by D'el-Rey Silva (1984, 1985); b—A 3-D schematic representation of the Caraíba mushroom (from D'el-Rey Silva et al., 1988); c—The overall pattern of F2×F3 interference for cross section 36 (see also the inset) is typical for sections 32–37 (the central part of the orebody). Diamond drill holes are indicated for different years. Adapted from D'el-Rey Silva et al. (1996) and D'el-Rey Silva and Oliveira (1999). See text for details.

The tonalite in the Airport outcrop is yellowish-grey, wellbanded, and composed of oligoclase-andesine, hornblende, biotite, orthopyroxene, clinopyroxene, minor microcline and quartz, with garnet, magnetite, apatite, and zircon as accessories. It also encloses cm- to dm-thick and N2 m-long bands of acid composition, as well as b1 m-sized lenses of nonporphyritic granitoid, all aligned parallel to S2, this one a quite homogeneous granulite-facies metamorphic banding consisting of ≤1 cm-thick bands of flattened crystals of feldspar, quartz, minor biotite, intercalated with ≤1 cm-thick bands of pyroxene, hornblende, plus biotite, and affected by numerous, 0.5–2.0 mscale, very tight F3 folds that plunge ≤25° to the S and are associated with a sub-vertical, N–S striking, and penetrative mineral foliation (S3) marked mostly by biotite, but also by hornblende plus quartz and feldspar. S3 can be seen crosscutting at very low angle the S1 banding in the boudins.

Only after the detailed mapping (Fig. 4), can the boudins be seen to define nearly E–W trending trails affected by F3 folds, revealing a more complete story: during D2 the G2 tonalite intruded continuous layers of E–W trending S1-foliated amphibolite.

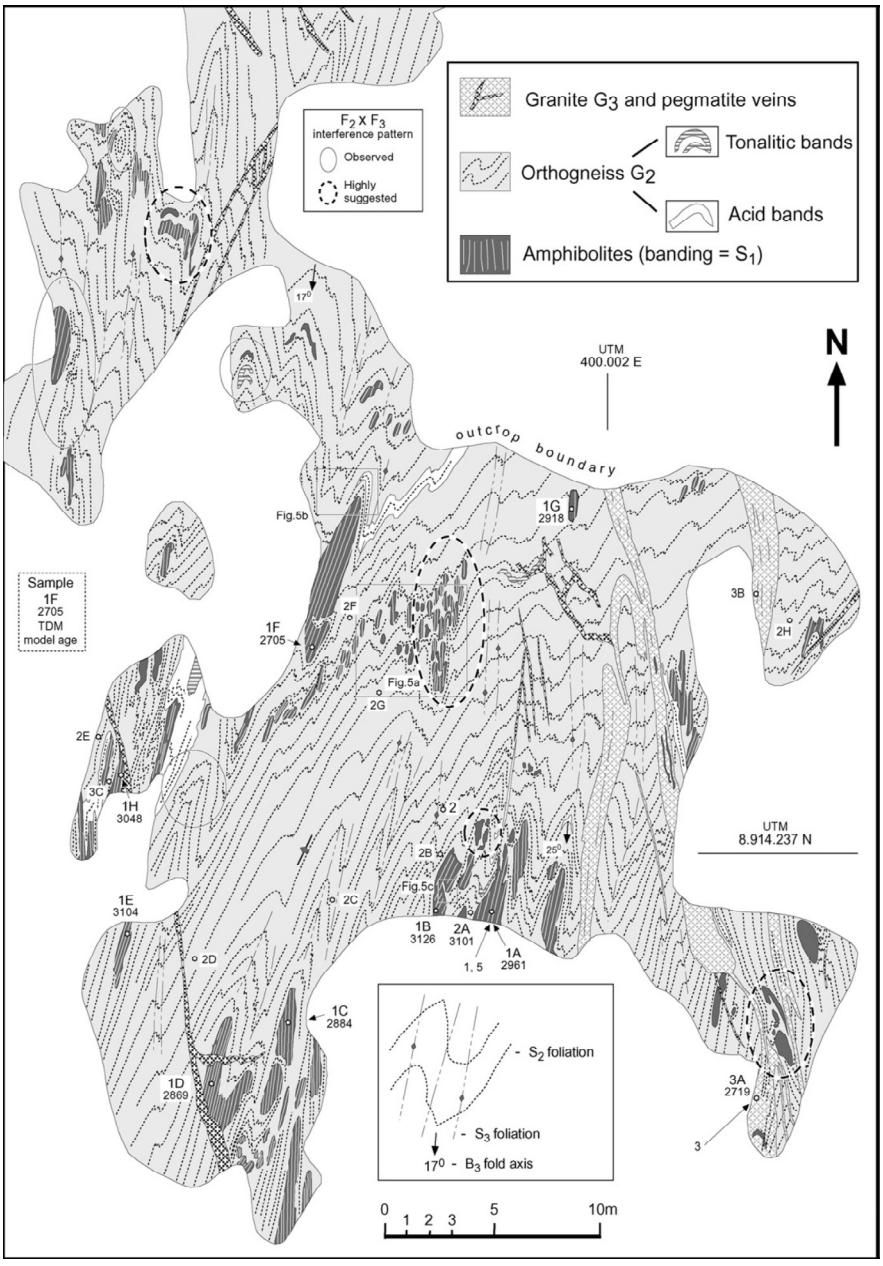

Fig. 4. Simplified geological map of the Caraíba Airport outcrop to show the site of collection of the samples used in this study. B3 fold axis plunges ≤25° to the S, whereas planar structures such as S1 in the amphibolite boudins, S2, andS3, all dip sub-vertically, unless in the very hinge of the F3 folds.G3 granite intrusions cut across some of the F3 hinges. Based on the original lithostructuralmapping at 1:100 scale carried with the aid of a plane table and alidade by L.J.H. D'el-Rey Silva and J.A.C. deMorais (D'el-Rey Silva, 1984, 1985). Figures indicative of F2×F3 interference pattern (some observed, other highly suggested) are indicated in the areas surrounded by ellipses. Details in text.

The amphibolite layers underwent boudinage while the tonalite deformed by ductile flow and acquired the granulite-facies S2 banding. During D3 the boudins rotated nearly 90° around a vertical axis, so their longer horizontal axis, originally oriented nearly E–W, became systematically oriented N–S, the boudin ellipses entrapped in the F3 hinges (Fig. 5a, b, e) and also underwent D3 shortening. The boudins systematically nested in the F3 hinges, with S1 and the long axis both parallel to S3, plus the abundant F2×F3 folding interference patterns in the tonalite, or highly suggested in the amphibolites (Fig. 4), altogether strongly support interpreting that: 1—S2 formed subparallel to S1; 2—the G2 tonalite is a syntectonic intrusion; 3—

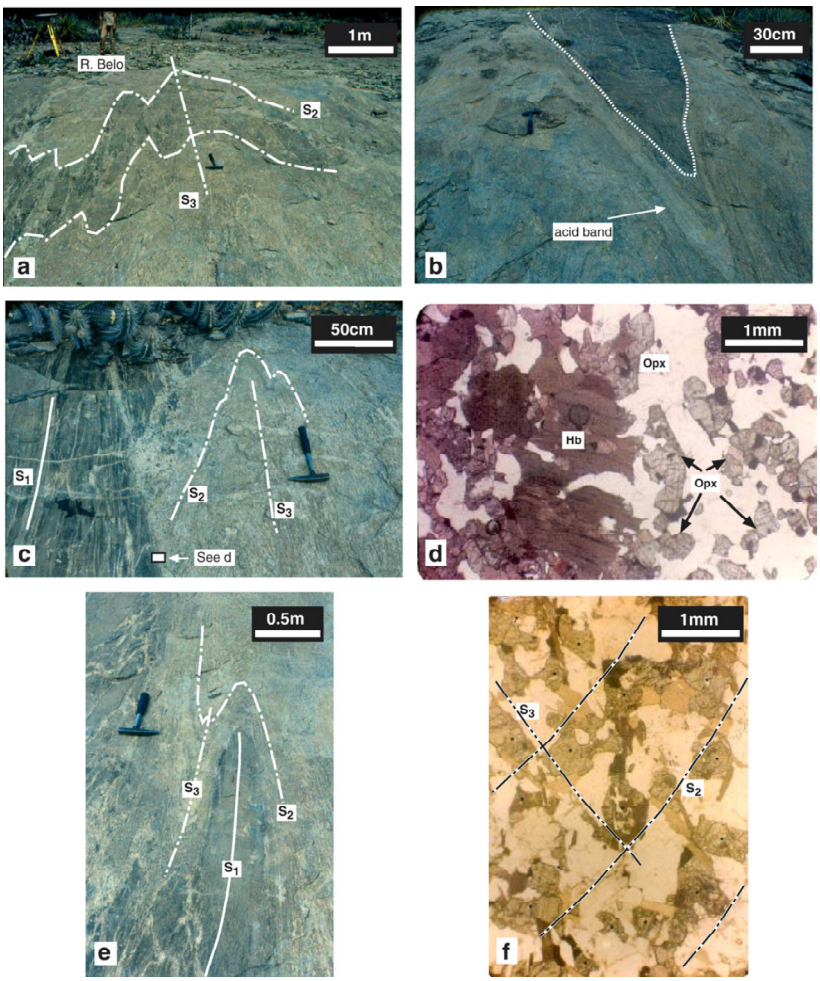

Fig. 5. Features of the Airport outcrop, as seen in four view to the S photos (a, b, c, e) and in two photos from thin-sections (d, f). Several boudins (a) define a E–W trending layer affected by F3 folds, in the central part of the outcrop. The longer axis of the boudins parallels the hammer's handle that points to the S. Technician R. Belo is partially shown on the upper left corner, beside the plane table and alidade used for detailed mapping; b — A 10 cm-thick acid band and the grey tonalite affected by an F3 fold around the northern margin of the largest boudin (dotted line) in the outcrop. The traces of S1 and AP3 are parallel one to each other; c — Relationships between the F3 folded tonalite and the eastern side of the boudin source of sample 1A. Note the b50 cm-wide felsic pegmatoid with over 1 cm-big crystals of

orthopyroxene along the amphibolite-tonalite contact; d—Detail of a thin section from sample collected at the boudin-tonalite contact (in c). Large crystals of hornblende (Hb) dominate in the left half of the picture, and occur together with plagioclase and some crystals of orthopyroxene (Opx), whereas the latter dominates in the right half, together with larger crystals of plagioclase. Opx crystals grew at the expenses of the Hb crystals along the margin of the boudin, as also demonstrated by circular crystals of Hb included in Opx (D'el-Rey Silva, 1984, 1985); e—Detail of a F3 fold affecting S2 around the head of a boudin. Note the traces of S1 (inside the boudin) and S3 both parallel to the boudin's long axis; and f—Picture of part of a thin-section beside a F3 hinge. Note crystals of pyroxene (some marked by *) and plagioclase along S2, as well as ribbons of biotite and flattened crystals of plagioclase defining the S3 foliation.

D1-D3 deformation was progressive; and 4 — lithological layers, as well as S1 and S2 foliation, may all have had an E–W trend somewhere in the Curaçá terrane, before D3 deformation. Thus, it is possible that the amphibolite layers where affected by E–W trending, 10–100 m sized, isoclinal F2 folding, in the hinges of which the G2 tonalite intruded. The double row of boudins in the central part of the outcrop (Fig. 4) suggests a 10 m-sized F2×F3 boomerang-like Type 2 interference pattern. The strength of interpreting and the validity of the U–Pb diffusion technique age data (next section) rely in the validity of these structural and metamorphism relationships demonstrated above, and also in the fact that such ages agree with others obtained for the same rocks, using more precise techniques, and are subject of a detailed discussion at the end of this paper.

U (ppm)	Pb (ppm)	Pb206 Pb204 (obs)	Pb207* U235	(pct)	Pb206* U238	(pct)	Correl. coeff. (rho)	Pb207* Pb206*	(pct)	Pb206* U238 Age (My)	Pb207* U235 Age (My)	Pb207* Pb206* Age (My)	(My)
145	76	1596	7.56206	0.57	0.37703	0.571	0.99019	0.145466	0.08	2062	2180	2293	1.4
196	71	862	6.36684	0.83	0.360684	0.791	0.94863	0.128025	0.263	1985	2027	2071	4.6
49	17	448	5.38241	1.24	0.311302	1.200	0.96828	0.125399	0.309	1747	1882	2034	5.5
205	32	297	1.40039	1.84	0.142056	1.650	0.90839	0.071497	0.769	856	889	971	16
201	74	815	6.32118	0.66	0.360535	0.636	0.966734	0.127160	0.168	1984	2021	2058	3
174	65	857	6.42752	0.68	0.363910	0.663	0.975212	0.128100	0.150	2000	2036	2072	2.6
546	202	604	5.99644	0.45	0.344294	0.431	0.959408	0.126317	0.128	1907	1075	2047	2.3
330	108	817	7.42198	1.04	0.287785	1.040	0.997556	0.1870470	0.729	1630	2163	2716	1.2
90	13	916	2.0111	1.02	0.145027	1.020	0.925758	0.1005740	0.383	873	1119	1634	7.2
577	116	7745	3.55528	0.5	0.201059	0.496	0.991762	0.1282480	0.063	1181	1539	2074	1.1
313	132	1116	7.57359	0.35	0.362173	0.349	0.994050	0.1516650	0.004	1992	2181	2364	0.65
206	100	582	8.57972	0.7	0.392694	0.633	0.906718	0.1584590	0.294	2135	2294	2439	5
309	84	383	2.9353	1.02	0.199033	0.994	0.977454	0.1069610	0.215	1170	1391	1748	4

Table 1 - Summary of the U–Pb data from thirteen fractions of zircons from 10 kg of the amphibolite

5. Geochronology

5.1. Sample population and analytical procedures

The isotopic data derive from eleven samples of rocks collected in the Airport outcrop (Fig. 4), then treated and analyzed in the Laboratory of Geochronology — University of Brasília. Zircon concentrates were extracted using conventional gravimetric (DENSITEST®) and magnetic (Frantz

isodynamic separator) techniques applied to ca. 10 kg rock samples collected in the largest boudin in the outcrop. Final purification was achieved by handpicking using a binocular microscope. For the conventional U–Pb analyses, fractions were dissolved in concentrated HF and HNO3 (HF:HNO3=4:1) using microcapsules in Parr-type bombs. A mixed 205Pb–235U spike was used. Chemical extraction followed standard anion exchange technique, using Teflon micro columns, following procedures modified from Krogh (1973). Pb and U were loaded together on single Re filaments with H3PO4 and Si gel, and isotopic analyses were carried out on a Finnigan MAT-262 multicollector mass spectrometer equipped with secondary electron multiplier—ion counting. Procedure blanks for Pb, at the time of the analyses, were better than 20 pg. PBDAT (Ludwig, 1993) and ISOPLOT-Ex (Ludwig, 2001a) were used for data reduction and age calculation. Errors for isotopic ratios are 2σ.

The Sm–Nd isotopic analyses followed the method described by Gioia and Pimentel (2000): whole rock powders (ca. 50 mg) were mixed with 149Sm–150Nd spike solution and dissolved in Savillex capsules. Sm and Nd extraction of whole-rock samples followed conventional cation exchange techniques, using teflon columns containing LN-Spec resin (HDEHP — di-ethylhexil phosphoric acid supported on PTFE powder). Sm and Nd samples were loaded on Re evaporation filaments of double filament assemblies and the isotopic measurements were carried out on a multi-collector Finnigan MAT 262 mass spectrometer in static mode. Uncertainties for Sm/Nd and 143Nd/144Nd ratios are better than ±0.4 % (1σ) and ±0.005% (1σ) respectively, based on repeated analyses of international rock standards BHVO-1 and BCR-1. 143Nd/144Nd ratios were normalized to 146Nd/144Nd of 0.7219 and the decay constant (λ) used was 6.54×10−12.

5.2. U–Pb geochronology of zircons from amphibolite

The dated basic rock consists of orthopyroxene, hornblende, plagioclase, clinopyroxene, biotite, and quartz. Two populations of zircons are distinguished, one comprising colourless, elongate, prismatic, and inclusion free crystals, the other consisting of clean, rounded, red to pink colour crystals.

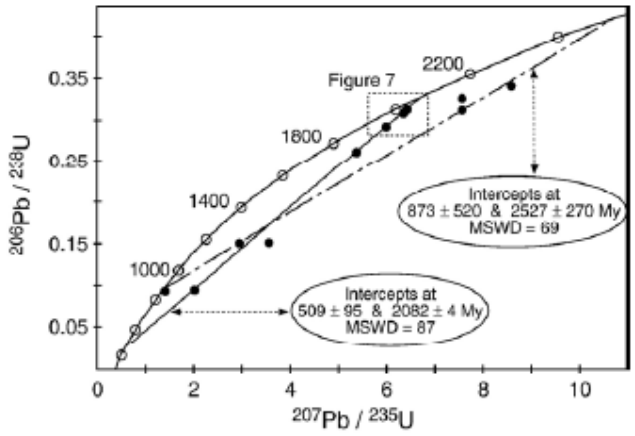

Fig. 6. U–Pb ages defined by plotting the data in Table 1 and relative to zircons from amphibolite in the largest boudin in the Airport outcrop. Details in text.

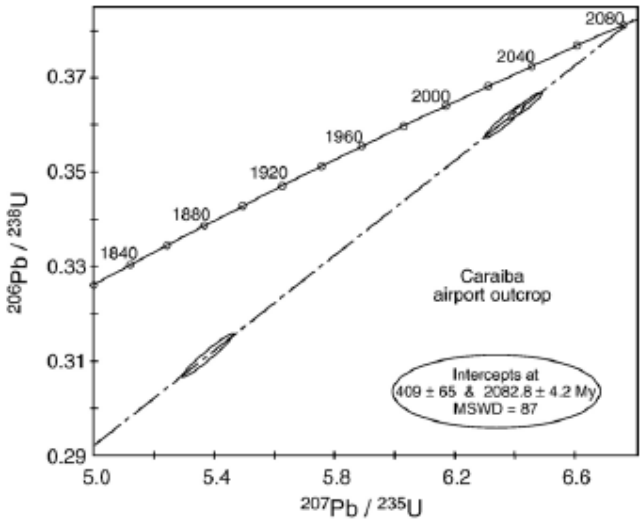

Fig. 7. Detail concordia diagram for the three points in the upper part of the diagram in Fig. 6, showing the accurate U–Pb age obtained for metamorphism M3 in the study outcrop. Details in text.

Table 1 contains a summary of the U–Pb data from the analyses of 13 fractions of grains of zircons. The concordia diagram for the analytical data shows considerable complexity in the U–Pb isotopic system, and the scattered plot of grains of zircons indicates large discordance with the lower and upper intercepts of the diagram (Fig. 6).

We interpret the colourless zircons as representative of the igneous protolith. Coincidently, their alignment provide the older U–Pb age of 2577±110 Ma among other possible regressions. In despite the large error, this age is similar to the most precise U–Pb SHRIMP age of 2580±10 Ma obtained by Oliveira et al. (2004) for Caraíba norite, suggesting contemporary magmatic events. The population of red-pink zircons (interpreted as metamorphic crystals) plots along another discordia and define an age of 2082±4 Ma that we accept as a good result (Fig. 7) for the regional M3 metamorphism, because it is very similar to crystallization ages of clearly syntectonic intrusions, such as G3 granites in the southern part of the Caraíba orebody (2051±16 Ma age, U–Pb from monazite; D'el-Rey Silva et al., 1996), and the Itiúba Syenite (2084±9 Ma U–Pb SHRIMP age; Oliveira et al., 2004). Points probably related to Pb loss plot very near to the lower intercept of the diagram, providing ages of 1.0 and 0.8 Ga that currently we speculate to be geologically meaningless.

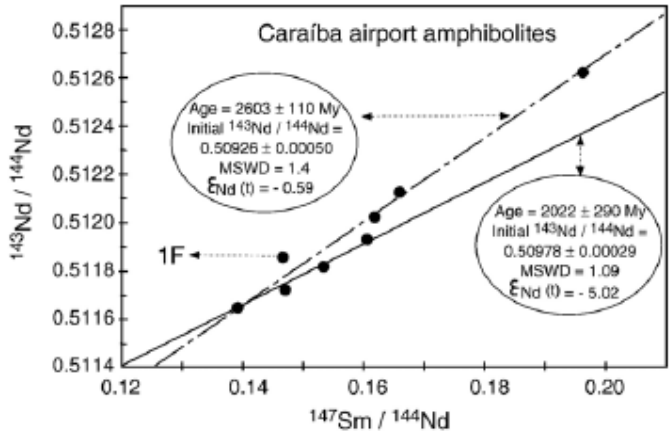

Fig. 8. Plotting the data from eight samples of amphibolite in Table 2 in the Sm–Nd diagram results in two isochronic ages. According to Frost and Frost (1995) the causes for moving points out of true isochronic lines may be due to: 1— Reequilibrium at outcrop scale that would move the points along the vertical axis (143Sm/144Nd ratio), then leading to a new isochronic straight line and affecting the original age of the protolith; 2 — Variation in the igneous protolith at the time of formation, a situation that would increase the 147Sm/143Nd ratio, changing the inclination of the lines without re-equilibration of the system; and 3 — Re-distribution of Sm relative to Nd during high-grade metamorphism, most likely to be the case in the Airport outcrop, as the process would generate parallel straight lines, but would not re-equilibrate the originally igneous data, therefore the ages will rather correspond to isochronic alignments.

5.3. Sm–Nd geochronology in the Airport outcrop

The systematic study of Nd isotopes was applied to ten samples: eight of them collected in different boudins of amphibolite (1A–H; Fig. 4), one sample of the G2 tonalite (2A), and one sample of the G3 granite (3A), all listed in Table 2.

The isotopic data of G2 tonalite [sample 2A:TDM=3101 Ma; εNd(t)=−6.79] and G3 granite [sample 3A:TDM=2719 Ma; εNd(t)=−9.87] suggest derivation from partial melting of Mesoarchean continental crust, likely to be the continental part of the basement of the Tanque Novo supracrustals. Plotted together in a single 143Nd/144Nd versus 147Sm/144Nd isochronic diagram (Fig. 8), the data from the eight samples of amphibolites, appear to define two isochrones. The older age of 2603±110 Ma, with εNd(t) values close to zero, is interpreted as the age of crystallization of the igneous protolith of the amphibolites. The younger age of 2022±290 Ma and the negative εNd(t) values are consistent with late isotopic reequilibration of the Nd isotopic system and partial reequilibrium of Nd isotopic system during regional metamorphism. This process could have been theoretically related to contaminating fluids with low Sm/Nd ratio (McCulloch and Black, 1984), or loss of Sm relative to Nd during metamorphism.

The values obtained for the Nd isotopes of individual samples of amphibolites indicate a heterogeneous isotope distribution reflected in varied TDM ages and variable values of $^{\varepsilon}Nd^{(t)}$ (Fig. 9), and we found this related to the size of the boudins. Samples with values of $^{\varepsilon}Nd^{(t)}$ close to zero, or slightly positive (1A, 1C, 1D, and 1H) were all from large boudins (Fig. 4) and are indicative of preservation of the igneous protolith's isotopic composition with TDM model ages around 2.7–2.8 Ga, whereas TDM model ages around 2.9–3.1 Ga correspond to samples from the border of a boudin (1B); or from small boudins (1E and 1G) with more fractioned Sm/Nd ratios and the most negative εNd(t) values that reflect larger isotopic interaction with the host rocks. Sample 1F (from the largest boudin; Fig. 4) displays the best preserved original composition and the highest positive value of $^{\varepsilon}Nd^{(t)}$.

Sample	Rock Type	Sm (ppm)	Nd (ppm)	$^{147}Sm/^{144}Nd$	$^{143}Nd/^{144}Nd \pm 2\sigma$	$\varepsilon_{(0)}$	T_{DM} (My)	$\varepsilon_{Nd}(t)$
1A	Amphibolite	1.94	7.08	0.1658	0.512124 (12)	−10.02	2961	+0.14
1B	Amphibolite	3.44	13.99	0.1487	0.511724 (09)	−17.83	3126	−2.03
1C	Amphibolite	2.82	8.76	0.1960	0.512619 (24)	−0.37	2884	−0.14
1D	Amphibolite	4.64	19.74	0.1393	0.511648 (17)	−19.31	2869	−0.42
1E	Amphibolite	5.10	20.19	0.1534	0.511816 (25)	−16.04	3104	−1.79
1F	Amphibolite	3.98	16.44	0.1466	0.511855 (32)	−15.28	2705	+1.21
1G	Amphibolite	4.59	17.37	0.1606	0.511930 (22)	−13.81	2918	−1.93
1H	Amphibolite	2.06	7.73	0.1616	0.512015 (23)	−12.15	3048	−0.60
2A	Tonalite (G_2)	7.24	35.39	0.1238	0.511241 (25)	−27.24	3101	−6.79
3A	Granite (G_3)	1.79	19.84	0.0548	0.510202 (19)	−47.52	2719	−9.87

Table 2 - Summary of the Sm–Nd data from the eight samples collected in the airport outcrop

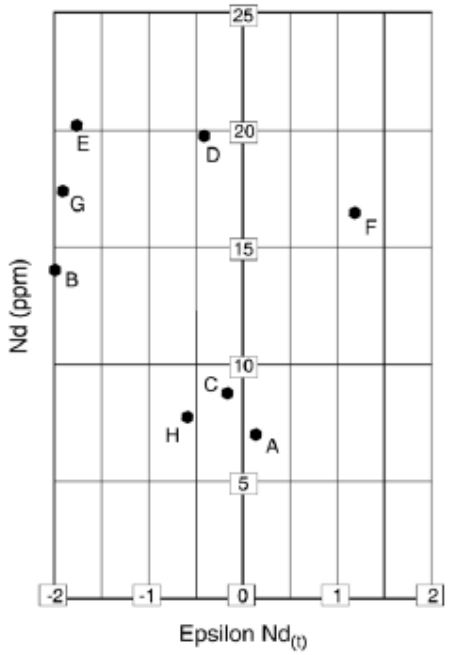

Fig. 9. $\varepsilon_{Nd}^{(t)}$×Nd content Cartesian graph constructed with data from samples 1A–H in Table 2.

6. Discussion

The isotopic data suggest that the geochemical signature of the amphibolites is compatible with basalts sourced from an initially depleted mantle. These, combined with the strongly similar ages of crystallization for Caraíba norites (Oliveira et al., 2004) and airport amphibolite (this paper) leads to consider that the protolith of the Caraíba orebody could have been either: a—basaltic oceanic crust; b — basalts shed as flows within sediments in the Tanque Novo sequence; or c—a gabbroic sill intruded into the Tanque Novo sequence. All these possibilities agree with the large inventory of data from the area surrounding Caraíba, and from the Curaçá terrane as a whole. This inventory requires that before D1 deformation the orebody's protolith was a conformable body in the same sub-horizontal position of the Tanque Novo

volcanic-sedimentary pile, so that all lithotypes above came to experience the same D1-D3 structural/metamorphic evolution.

The age of M1 metamorphism has not been determined. However, once the field relationships in the Airport outcrop indicate a progressive evolution similar to the one observed in the Caraíba orebody, and the observation that the G2 intruded syntectonically, all support the interpretation that the structural and metamorphic evolution of the Curaçá terrane may be bracketed between (2.35?)2.3–2.25 and 2.05 Ga (D'el-Rey Silva et al., 1996), with cooling lasting until 1900 Ma ago. The new ages described in this paper suggest a more detailed scenario: M2 granulite facies conditions peaked in the 2250– 2200 Ma interval, whereas M3 amphibolite facies conditions peaked at 2080–2050 Ma interval (Fig. 10).

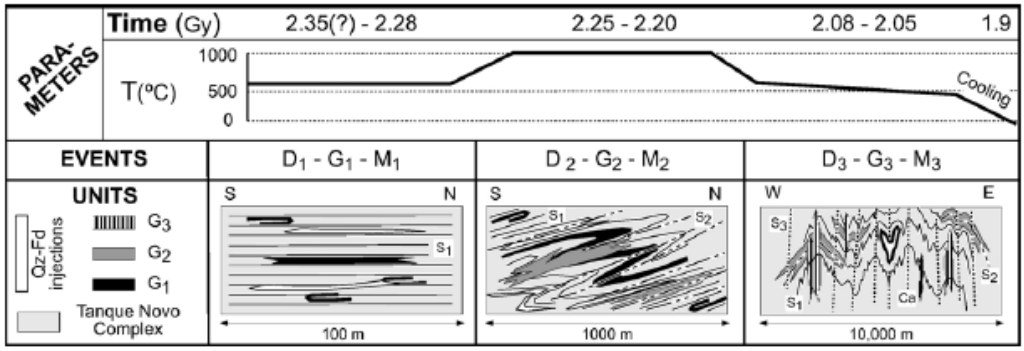

Fig. 10. Summary diagrams for the tectonic evolution of the Curaçá belt. D1-D3 structures are observed since cm- to dm-scale up to the scale indicated below each diagram. The leftmost diagram displays G1 conformable bodies in the Tanque Novo Complex, all affected by S1 and intrafolial F1 folds. M1 metamorphism probably peaked in the 2.3–2.8 Gy interval. The 2.58 Gy old body (Oliveira et al., 2004) destined to be the Caraíba orebody is depicted in the center, with no implication on the origin of the protolith. The central diagram displays S2 and asymmetric F2 folds affecting previous units and structures, as well as syntectonic G2 intrusions, all associated to M2 metamorphism (T≤1000 ºC; Leite, 2002) peaked in the 2.25–2.20 Gy interval (this paper). The diagram to the right shows D1–D2 units and structures affected by F3 folds and S3, and intruded by G3 bodies, all affected by M3 metamorphism peaked 2.08–2.05 Gy ago (our result combined with data in D'el-Rey Silva et al., 1996; Oliveira et al., 2004). Final cooling lasted until ~1.9 Gy ago. The Caraíba mushroom is to the left of the Curaçá antiform (Ca). Temperatures around 600 ºC for M1 and M3 fit data in Leite (2002) for amphibolite facies metamorphism in his PhD study area.

Three similarly important facts make the Curaçá belt a classical area for tectonic analysis based on the combination of accurate field geology, detailed structural observations, and careful isotope analysis of different systems.

Firstly, the large errors associated with the ages in here indicate open-system behaviour of the U–Pb and Sm–Nd isotopic systems in the amphibolite protolith. The difficulty of dating basic rocks in a high grade terrane resides in

that such rocks contain extremely small volumes of minerals suitable for high precision age determinations, and their isotopic systems are commonly affected at varied intensities during severe metamorphism, so the study of these systems will indicate varied levels of complexity, no matter if the tectonic evolution was polyphase or polycyclic (Frost and Frost, 1995; Gruau et al., 1996; Pidgeon and Wilde, 1998; Carson et al., 2002).

Secondly, the older cratonic blocks in the São Francisco Craton preserve different isotopic ratios (Fig. 1a) acquired before the Paleoproterozoic. The I–S–C orogen may involve multiple collisions along the margins of the Gavião and Serrinha Mesoarchean blocks during the Neoarchean and Paleoproterozoic collisions, and unravelling these presents a considerable challenge.

In the area south of the Itiúba syenite, Teixeira (1997) mapped the Caraíba and Tanque Novo (or Tanque Novo-Ipirá) complexes folded/tectonically imbricate together with the São José do Jacuípe Suite, a unit consisting of norites, gabbronorites, gabbros, peridotites, and pyroxenites, and suggested that part of the Caraíba Complex defines a magmatic arc, subsequently dated as Neoarchaean (quoted in Delgado et al., 2003), whereas part of the two other units matches the characteristics of oceanic crust. The interpretation here that the Airport outcrop may preserve 2.6 Ga oceanic crust fits this model well.

The third fact is that the long-lived and transpressionrelated tectonics recorded in the I–S–C orogen has a great potential to transform a single suture into a stack of subvertical suture segments, and the traces of these segments may spread over a wider field area than the original suture zone. In case of polycyclic evolution, this tectonic scenario could have stacked segments of two collision sutures, creating a true geological puzzle.

We are aware that other regressions are possible with our U– Pb data. However, the U–Pb age of 2.6 Gy for the amphibolite protolith is sustained here because: a — it is the highest value obtained; b — it derives from the population of clean zircons; c—it is within error of the Sm–Nd isochronic age we obtained for the same amphibolites; and d—both ages above are similar to the SHRIMP age obtained for the Caraíba norite (Oliveira et al., 2004). Metamorphic zircons

in the amphibolites yield an age between 2.3 to 2.2 Ga. We suggest that the 2.3–2.2 Ga interval is the time in which the isotopic system in the amphibolites was disturbed by incoming fluids derived from the G2 tonalite, and sustain the interpretation based on two facts: 1 — the G2 tonalite is a syn-tectonic intrusion; and, 2 — pristine zircons from the G2 tonalite in the same Airport outcrop provided an age of 2248±36 Ma (D'el-Rey Silva et al., 1996), emphasizing the significance of this early Paleoproterozoic D2 event.

Combining our results with those of previous workers, we propose the following scenario for the tectonic evolution of the region. The protoliths to the Airport amphibolites and the Tanque Novo sequence, both formed ~2.6 Ga, when a wide ocean separated the Gavião and Serrinha blocks. The Caraíba Complex was evolving in this ocean as an island arc above an east-dipping subduction zone that plunged below the Serrinha Block (Leite, 2002). M1 amphibolite facies metamorphism (our results) peaked sometime between 2.35–2.80 Ga, as the rocks entered in the subduction zone, then underwent layer-parallel shearing, and acquired D1 structures. D2 Structures developed as the rocks were buried further, and the E–W fold axes (F2) formed by differential flow affecting fold axes originally trending N–S, a kind of embayment process pointing-down to the east, inside the N–S trending subduction zone and coeval with granulite facies metamorphism (M2). This metamorphism condition peaked at 2.25–2.2 Ga, our result that on one hand fits in the (2.2–2.1 Ga) interval suggested by Leite (2002) for amalgamation of the island arc to the Serrinha Block, and on the other hand, also suggests a back-arc scenario for part of the Tanque Novo sequence as well as for the amphibolites and the Cu-mineralized orebodies (see also Bello, 1986). Closure of the ocean at ~2.1 Ga resulted in the formation of a foreland basin to the west (all in Leite, 2002). The roots of the orogen started to be uplifted as the subduction zone was choked when the Gavião Block began to enter into the subduction zone, and the ultimate Gavião – Serrinha continental collision at 2.08 Ga (Leite, 2002) caused D3 deformation under M3 amphibolite facies metamorphic conditions peaked at 2.08–2.5 Ga throughout the I–S–C orogen.

7. Conclusions

This paper has brought to light new U–Pb and Sm–Nd geochronology data obtained after detailed studies carried out in amphibolites (mainly), G2 tonalite, and G3 granite of the Airport outcrop, situated ~5 km to the north of the Caraíba Cu-orebody, in the Curaçá terrane, northern São Francisco Craton, Brazil. The new data, coupled with well-known tectonic structures and other field data from the Airport outcrop, clearly imply D1-D3 progressive deformational events under amphibolite-granuliteamphibolite M1-M3 metamorphism, and G1-G3 magmatism. The G2 tonalite and G3 granite in the Airport outcrop derive (Sm–Nd data) from partial melting of a Mesoarchean continental crust existing in the Curaçá terrane. This Mesoarchean crust is likely to be part of the basement of the Tanque Novo supracrustals. The igneous protolith of the amphibolites in the outcrop is Neoarchean and crystallized ca. 2600 Ma ago (U–Pb and Sm–Nd data). This may be also in the age-interval of sedimentation in the northern part of the basin precursor of the Itabuna-Salvador-Curaçá orogen. Granulite facies metamorphism (M2) and amphibolite facies metamorphism (M3) in the Curaçá terrane are respectively dated around 2250–2200 Ma, and 2084–2050 Ma (U–Pb data). The progressive evolution supports previous interpretation that M1 amphibolite facies metamorphism (still lacking a direct age determination) is as old as 2300 Ma.

However, the progressive evolution recorded in the Curaçá terrane as a whole does not rule out the possibility that other parts of the Curaçá terrane, or elsewhere in the I–S–C orogen, still hide evidence for a polycyclic evolution. The results in here emphasize the importance of combining geochronology, lithostructural and metamorphic detailed studies of key outcrops for unravelling the evolution of high-grade terrains, and constitute a contribution for the geochronology approach of high-grade terranes in general.

Acknowledgements

Dr. Sérgio L. Junges is thanked for support during isotopic analyses at the Geochronology Lab — UnB. Elton L. Dantas thanks CNPq for grant 471144/03-7. The first author dedicates his part in this work to his wife and sons, and to the memory of geologist José Genário de Oliveira (deceased in 2000), an enthusiastic of the Caraíba Project, who largely facilitated the visit to

the mine and collection of the samples in the Airport outcrop. Two anonymous reviewers are thanked for excellent comments that helped to make better this piece of work. Dr. Alan Collins (The University of Adelaide, Australia) is deeply acknowledged for his superb help on final editing. This paper is a contribution to IGCP project 509, Palaeoproterozoic Supercontinents and Global Evolution.

References

Ackermand, D., Herd, R.K., Reinhardt, M.C., Windley, B.F., 1987. Sapphirine parageneses from the Caraíba Complex, Bahia, Brazil: the influence of Fe2+–Fe3+ distribution on the stability of Sapphirine in natural assemblages. Journal of Metamorphic Geology 5, 323–339.

Barbosa, J.S.F., 1996. O embasamento Arqueano e Proterozóico Inferior de Estado da Bahia. In: Barbosa, J.S.F., Dominguez, J.M.L. (Eds.), Geologia da Bahia, Texto Explicativo SME-SGM, Capítulo III, pp. 63–83.

Barbosa, J.S.F., Sabaté, P., Dominguez, J.M.L., 1996. O estado da Bahia na Plataforma Sul-Americana, suas sub-divisões, critérios de empilhamento estratigráfico das coberturas plataformais e ciclos geotectônicos. In: Barbosa, J.S.F., Dominguez, J.M.L. (Eds.), Geologia da Bahia, Texto Explicativo SME-SGM, Capítulo II, pp. 41–61.

Barbosa, J.S.F., Sabaté, P., 2002. Geological features and the aleoproterozoic collision of four Archean crustal segments of the São Francisco Craton,

Bahia, Brazil. Anais da Academia Brasileira de Ciencias 74 (2), 343–359.

Barbosa, J.S.F., Sabaté, P., 2004. Archean and Paleoproterozoic crust of the São Francisco Craton, Bahia, Brazil: Geodynamic Features. Precambrian Research 133, 1–27.

Bello, R.M.S., 1986. Jazida de Cobre de Surubim, Vale do Curacá, Bahia: Mineralogia, Petrografia e Petrogênese. Ph.D. thesis, University of São Paulo (USP).

Carson, J.C., Ague, J.J.A, Grove, M., Coath, D.C., Harrison, M.T., 2002. U–Pb isotopic behaviour of zircon during upper-amphibolite facies fluid infiltration in the Napier Complex, east Antarctica. Earth and Planetary Science Letters 199, 287–310.

Condie, K.C., 1989. Plate Tectonics and Crustal Evolution, Third ed. Pergamon Press, Oxford-UK.

D'el-Rey Silva, L.J.H., 1984. Geologia e controle estrutural do depósito cuprífero Caraíba, Vale do Curaçá, Bahia, Brasil. M.Sc. thesis, Federal University of Bahia (UFBa).

D'el-Rey Silva, L.J.H., 1985. Geologia e controle estrutural do depósito cuprífero Caraíba, Vale do Curaçá, Bahia. Geologia e Recursos Naturais do Estado da Bahia, SME, Série Textos Básicos 6, 51–123.

D'el-Rey Silva, L.J.H., 1993. Geologia Estrutural e Tectônica na área do Projeto Lajedinho-Ipirá. Consulting report for CBPM, Salvador, 23 pp., 23 figures.

D'el-Rey Silva, L.J.H., Oliveira, J.G., 1999. Geology of the Caraíba Copper Mine and its surroundings in the Paleoproterozoic Curaçá Belt- Curaçá River Valley, Bahia, Brazil. In: da Silva, M. da G., Misi, A. (Coordenadores) Base metal Deposits of Brazil, MME/CPRM/DNPM, 25-32.

D'el-Rey Silva, L.J.H., Cavalcante, P.R.B., Mota, E.R., Rocha da, A.M.R., 1988. Controle estrutural da mina de cobre Caraiba: implicações na lavra e na tectônica das faixas móveis do Proterozóico Inferior. XXXV Congresso Brasileiro de Geologia, Belém, Brazil, Anais SBG, vol. 1, pp. 16–29.

D'el-Rey Silva, L.J.H., Oliveira, J.G., Lima e Silva, F.J., 1994. The Mushroomshaped Caraíba Cu-deposit, Vale do Curaçá-Ba: Understanding the Structural Evolution of the Paleoproterozoic, Granulitic Ipirá-Curaçá Belt within the São Francisco Craton. XXXVIII Congresso Brasileiro de Geologia, Camboriú, Brazil, SBG, Boletim de Resumos Expandidos, vol. 2, pp. 175–177.

D'el-Rey Silva, L.J.H., Oliveira, J.G., Gaál, E.G., 1996. Implication of the Caraíba Deposit's structural controls on the emplacement of the Cu-bearing hypersthenites of the Curaçá Valley, Bahia-Brazil. Revista Brasileira de Geociências 26 (3), 181–196.

Delgado, I. de M., Souza, J.D., 1975. Projeto cobre Curaçá. Geologia Econômica do Distrito Cuprífero do Rio Curaçá — Bahia, Brasil. CPRM/DNPM, internal report, 30 volumes.

Delgado, I. de M., de Souza, J.D., da Silva, L.C., Silveira Filho, N.C., dos Santos, R.A., Pedreira, A.J., Guimarães, J.T., Angelim, L.A. de A., Vasconcelos, A.M., Gomes, I.P., de Lacerda Filho, J.V., Valente, C.R., Perrotta, M.M., Heineck, C.A., 2003. Geotectonics of the Atlantic Shield. Geology, Tectonics and Mineral Resources of Brazil: Text, Maps, and GIS, CPRM, pp. 227–334. 692 p., Chapter V.

Figueiredo, M.C.H., 1981. Geoquímica da rochas metamórficas de alto grau do nordeste da Bahia-Brazil. Geologia e Recursos Naturais do Estado da Bahia, SME, Série Textos Básicos 4, 1–71.

Frost, C.D, Frost, B.R., 1995. Open-system dehydration of amphibolites, Morton Pass, Wyoming: elemental and Nd and Sr isotopic effects. The Journal of Geology 103, 269–284.

Gáal, E.G., 1982. Evaluation of geological, geophysical, and geochemical data of the Curaçá Valley, and the Mundo Novo-Uauá-Rio Capim area. Consulting report for the Mineração Caraíba Ltda, MID-066/82.

Gioia, S.M.L., Pimentel, M.M., 2000. The Sm–Nd method in the geochronology laboratory of the University of Brasilia. Anais da Academia Brasileira de Ciencias 72, 219–245.

Gromet, L.D., 1991. Direct dating of deformational fabrics. In: Heaman, L., Ludden, J.N. (Eds.), Short Course Handbook on Applications of Radiogenic Isotope Systems to Problems in Geology. Mineralogists Association of Canada, pp. 167–192. Chapter 5.

Gruau, G., Rosing, M., Bridgwater, D., Gill, R.C.O., 1996. Resetting of Sm–Nd systematics during metamorphism of N3.7 Gy rocks: implications for isotopic models of early Earth differentiation. Chemical Geology 133, 225–240.

Hasuy, Y., D'el-Rey Silva, L.J.H., Lima e Silva, F.J., Mandetta, P., deMoraes, J.A., Oliveira, J.G.,Miola,W., 1982. Geology and copper mineralization of Curaçá River Valley, Bahia. Revista Brasileira de Geociências 12 (1-3), 463–474.

Inda, H.A.V., Barbosa, J.S.F., 1978. Mapa geológico do Estado da Bahia, escala 1:1.000.000. Texto explicativo. SME/CPM.

Jardim de Sá, E.F., Arcanjo, C.J., Legrand, J.-M., 1982. Structural and metamorphic history of part of the high-grade terrane in the Curaçá Valley, Bahia, Brazil. Revista Brasileira de Geociências 12, 251–262.

Krogh, T.E., 1973. A low-contamination method for hydrothermal decomposition of zircon and extraction of U and Pb for isotopic age determinations. Geochimica et Cosmochimica Acta 37, 485–494.

Leite, C.M.M., 2002. A Evolução Geodinâmica da Orogênese Paleoproterozóica nas Regiões de Capim Grosso-Jacobina e Pintadas-Mundo Novo (Bahia-Brasil): Metamorfismo, Anatexia Crustal e Tectônica. Ph.D. thesis, Federal University of Bahia (UFBA).

Leite, C.M.M., Barbosa, J.S.F, Nicollet, C., Kienast, J.R., Fuck, R.A., 2005. Ultrahigh-temperature metamorphism of sapphirine-bearing granulite from the 2.0 Gy Itabuna-Salvador-Curaçá orogen, Bahia, Brazil. III Sympósio sobre o Cráton do São Francisco, Salvador, Brasil, AnaisISSN :1808-6047, pp. 83–86.

Lindenmayer, Z.G., 1981. Evolução geológica do Vale do Curaçá e dos corpos máfico-ultramáficos mineralizados a cobre. M.Sc. thesis, Federal University of Bahia (UFBa).